



Article

# Performance Improvement for Mixed RF–FSO Communication System by Adopting Hybrid Subcarrier Intensity Modulation

Ting Jiang <sup>1</sup>, Lin Zhao <sup>1</sup> , Hongzhan Liu <sup>1,2,\*</sup>, Dongmei Deng <sup>1,2</sup>, Aiping Luo <sup>1,2</sup>, Zhongchao Wei <sup>1,2</sup>  and Xiangbo Yang <sup>1,2</sup>

<sup>1</sup> Guangdong Provincial Key Laboratory of Nanophotonic Functional Materials and Devices, Guangzhou 510006, China

<sup>2</sup> School of Information and Optoelectronic Science and Engineering, South China Normal University, Guangzhou 510006, China

\* Correspondence: lhzscnu@163.com

Received: 23 July 2019; Accepted: 4 September 2019; Published: 6 September 2019



**Abstract:** The improvement for hybrid radio frequency–free space optical (RF–FSO) communication system in wireless optical communications has acquired growing interests in recent years, but rarely improvement is based on hybrid modulation. Therefore, we conduct a research on end-to-end mixed RF–FSO system with the hybrid pulse position modulation–binary phase shift keying–subcarrier intensity modulation (PPM–BPSK–SIM) scheme. The RF link obeys Rayleigh distribution and the FSO link experiences Gamma–Gamma distribution. The average bit error rate (BER) for various PPM–BPSK–SIM schemes has been derived with consideration of atmospheric turbulence influence and pointing error condition. The outage probability and the average channel capacity of the system are discussed as well. Simulation results indicate that the pointing error aggravates the influence of atmospheric turbulence on the channel capacity, and the RF–FSO systematic performance is improved obviously while adopting PPM–BPSK–SIM under strong turbulence and severe pointing error conditions, especially, when the system average symbol length is greater than eight.

**Keywords:** free space optical (FSO); pulse position modulation–binary phase shift keying–subcarrier intensity modulation (PPM–BPSK–SIM); bit error rate (BER); pointing error; average symbol length

## 1. Introduction

In the past ten years, the hybrid radio frequency–free space optical (RF–FSO) communication system has attracted great interest due to its advantages compared with FSO system and RF system, respectively. RF system has the advantage of being insensitive to atmospheric turbulence, but the spectrum resource it requires is in shortage. On the contrary, features of the FSO system include license-free transmission, cost-effectiveness, and high security, which meet the demands of modern optical communication, but its communication quality is easily disturbed by the atmosphere [1,2]. The hybrid RF–FSO system could combine the advantages of the RF system and the FSO system [3]. Inevitably, dynamic weather and complex environment still affect the performance of hybrid RF–FSO system. Therefore, not only should a suitable channel model be chosen for hybrid RF–FSO system but also appropriate modulations could be adopted to improve the performance of the hybrid RF–FSO system.

Considering impacts of atmosphere including turbulence, pointing error, and pass fading, many channel models have been used to describe the hybrid RF–FSO system. Such as Nakagami-m/Gamma–Gamma distribution [4], Rayleigh distribution and M-distributed distribution [5],  $\kappa - \mu/\eta - \mu$

distribution and Gamma–Gamma distribution [6], and the Nakagami-m/Exponentiated Weibull (EW) distribution [7]. However, many studies adopted Rayleigh/Gamma–Gamma distribution [8–10], because the Gamma–Gamma distribution has a good simulation for the atmospheric turbulence from weak to strong of the FSO link, and Rayleigh distribution is close to the condition of the RF channel. As a result, we adopted Rayleigh distribution for the RF link and Gamma–Gamma distribution for the FSO link.

On the other hand, many previous researchers have focused on using different modulations to improve the mixed RF–FSO systematic performance for the modulation has a direct relationship with bit error rate (BER), which is a significant indicator to evaluate system performance. In reference [11,12], various pulse position modulation (PPM), binary phase shift keying (BPSK), and hybrid pulse position modulation–binary phase shift keying–subcarrier intensity modulation (PPM–BPSK–SIM) schemes have been analyzed on the performance over FSO link, the conclusion is that hybrid PPM–BPSK–SIM outperformed BPSK in single FSO link. In literature about the hybrid RF–FSO system [13,14], most of them adopted various binary modulation when it refers to the average bit error rate, BPSK is the most discussed as the binary modulation for it has the lowest bit error rate. In reference [4], authors investigated various PSK modulation and various quadrature amplitude modulation (QAM) in hybrid RF–FSO system. Unlike the FSO system [15], there are few studies on how to improve the hybrid RF–FSO system performance by adopting hybrid modulation, especially for the research of PPM–BPSK–SIM.

Motivated by the aforementioned studies, we investigated end-to-end performance of hybrid RF–FSO system with application of hybrid PPM–BPSK–SIM. The RF link follows Rayleigh distribution, the FSO link obeys Gamma–Gamma distribution, not only atmospheric turbulence but also pointing error is taken into consideration, and the system adopts various hybrid PPM–BPSK–SIM, the receiver employs intensity modulation/direct detection (IM/DD). The unconditional bit error rate (BER) of the PPM–BPSK–SIM is derived, it is noteworthy that the application of hybrid PPM–BPSK–SIM does bring optimization to the hybrid RF–FSO system performance from simulation results. The impact of pointing error on systematic performance is also discussed in detail.

The content of the article is arranged as follows. Specific information of the hybrid RF–FSO system and the channel model is described in Section 2. We derived the outage probability, the unconditional BER, and average channel capacity of the hybrid system in Section 3. The simulation is realized by MATLAB, and the results and discussion are shown in Section 4. Section 5 contains concluding remarks.

## 2. System and Channel Model

We consider an end-to-end hybrid RF–FSO system, it mainly consists of three parts—a source and a destination with a relay between them, the system model is shown below in Figure 1. The signal is received by the relay from the source through the RF channel, which obeys Rayleigh distribution. Considering the relatively lower implementation complexity [16], we adopt a fixed-gain amplify-and-forward (AF) relay which amplifies the RF signals and forwards them to next node directly [12]. In other words, the received RF signal will be transformed into an optical signal by the relay using the SIM technique, and the optical signal will be amplified by a fixed gain,  $G$ . After that, it is transmitted to the destination through the FSO link, which is supposed to obey Gamma–Gamma distribution, and IM/DD is used as the detection method in the destination.

The received signal of the relaying and the destination can be expressed  $y_1 = h_1x + n_1$  and  $y_2 = h_2y_1 + n_2$ , so the comprehensive expression is  $y_2 = h_2(h_1x + n_1) + n_2$ , where  $y_1$  and  $y_2$  denote the received signal,  $x$  represents the normalized signal from signal source,  $h_1$  and  $h_2$  are the channel coefficient of the RF link and the FSO link, respectively.  $h_2 = IG\eta$ , where  $I$  represents the irradiance intensity of FSO channel,  $G$  denotes the fixed gain of relaying scheme, and  $\eta$  represents the conversion coefficient of electrical-to-optical.  $n_1$  and  $n_2$  are additive white Gaussian noise (AWGN) with  $\sigma_1^2$  and  $\sigma_2^2$  as variance and mean of zero.

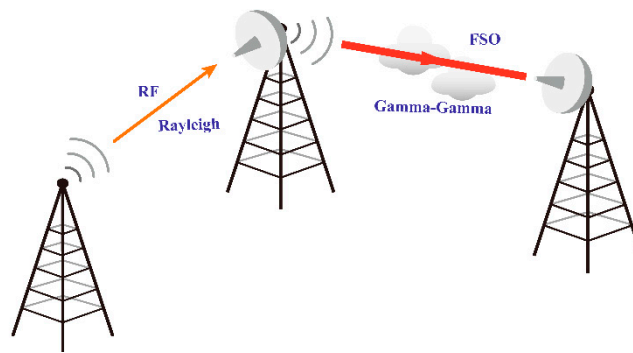


**Figure 1.** End-to-end mixed radio frequency (RF) and free space optical (FSO) communication system.

The RF link follows Rayleigh distribution in the hybrid RF–FSO system, the probability density function (PDF) of the RF link could be given as  $f_{\gamma_1}(\gamma_1) = \frac{1}{\gamma_1} \exp\left(-\frac{\gamma_1}{\bar{\gamma}_1}\right)$ , where  $\gamma_1$  represents the instantaneous signal to noise ratio (SNR) of the RF link and  $\bar{\gamma}_1$  denotes the average SNR in the RF channel. Using the definition of the cumulative distribution function (CDF),  $F_1 = \int_0^{\gamma_1} f_{\gamma_1}(\gamma) d\gamma_1$ . Hence, the CDF of the Rayleigh distribution can be expressed as  $F_1(\gamma_1) = 1 - \exp\left(-\frac{\gamma_1}{\bar{\gamma}_1}\right)$ .

The FSO link obeys Gamma–Gamma distribution with consideration of pointing error and atmospheric turbulence. The PDF of the SNR in FSO link can be given by [14,17–22]:

$$f_{\gamma_2}(\gamma_2) = \frac{\xi^2}{2\gamma_2\Gamma(\alpha)\Gamma(\beta)} \times G_{3,0}^{1,3} \left( \alpha\beta \sqrt{\frac{\gamma_2}{\bar{\gamma}_2}} \left| \begin{matrix} \xi^2 + 1 \\ \xi^2, \alpha, \beta \end{matrix} \right. \right), \tag{1}$$

where  $\gamma_2$  represents the instantaneous SNR of the FSO hop,  $\bar{\gamma}_2$  is the average SNR in the FSO channel,  $\alpha$  and  $\beta$  are the fading parameters that can reflect turbulence conditions.  $\xi = \frac{\omega_e}{2\sigma_s}$ ,  $\xi$  is the pointing error parameter, which is determined by the pointing error displacement standard deviation at the destination and equivalent beam radius (i.e., when  $\xi \rightarrow \infty$ , we get a case without influence of pointing error, the pointing error can be ignored).  $\Gamma(\cdot)$  is the Gamma function and  $G(\cdot)$  is the Meijer’s G function, and 3, 0, 1, 3 are the parameters associated with the Meijer’s G function, they are defined in reference [23]. Using the same method as in RF link, the CDF of the Gamma–Gamma distribution with the influence of pointing error can be given by [24,25]:

$$F_2(\gamma_2) = \int_0^{\gamma_2} f_{\gamma_2}(\gamma_2) d\gamma_2 \tag{2}$$

$$= \frac{\xi^2}{2\gamma_2\Gamma(\alpha)\Gamma(\beta)} G_{3,1}^{2,4} \left[ Z \left| \begin{matrix} 2, \xi^2 + 1 \\ \xi^2, \alpha, \beta, 1 \end{matrix} \right. \right],$$

where  $Z = \frac{\alpha\beta\gamma_2}{\sqrt{\bar{\gamma}_2}}$ .

Considering the relay with fixed gain, the signal will be amplified with a fixed relay gain,  $G$ , and forwarded to the destination. Hence, the end-to-end instantaneous SNR of the mixed RF–FSO system could be expressed as  $\gamma = \frac{\gamma_1\gamma_2}{\gamma_2+C}$ , where  $C$  is a constant associated with  $G$  [26].

The CDF of the hybrid RF–FSO system is defined as [9]:

$$F_\gamma(\gamma) = \Pr\left(\frac{\gamma_1\gamma_2}{\gamma_2+C} < \gamma_{th}\right) \tag{3}$$

$$= \int_0^\infty \Pr\left(\frac{\gamma_1\gamma_2}{\gamma_2+C} < \gamma_{th} | \gamma_2\right) f_{\gamma_2}(\gamma_2) d\gamma_2$$

$$= \int_0^\infty F_1\left(\frac{\gamma_{th}(\gamma_2+C)}{\gamma_2}\right) f_{\gamma_2}(\gamma_2) d\gamma_2.$$

Using  $\Gamma(g, x) = \int_0^x t^{g-1} e^{-t} dt$ , the CDF of Rayleigh distribution, and Equation (3), the CDF of the hybrid RF-FSO system is

$$F_\gamma(\gamma) = 1 - \frac{2^{(\alpha+\beta)} A \sqrt{C}}{16\pi \sqrt{\gamma_1}} \sqrt{\gamma} \exp\left(-\frac{\gamma}{\gamma_1}\right) \times G_{6,0} \left( \frac{(\alpha\beta)^2 C \gamma}{16\gamma_1 \gamma_2} \middle| \frac{\xi^2+1}{2} \right)_{\kappa_1} \quad (4)$$

where  $A = \alpha\beta\xi^2 / (2\sqrt{\gamma_2}\Gamma(\alpha)\Gamma(\beta))$  and  $\kappa_1 = \frac{\xi^2-1}{2}, \frac{\alpha-1}{2}, \frac{\alpha}{2}, \frac{\beta-1}{2}, \frac{\beta}{2}, -\frac{1}{2}$ .

### 3. Performance Analysis

#### 3.1. Outage Probability

Outage probability is the probability that the instantaneous SNR,  $\gamma$ , is smaller than the threshold value  $\gamma_{th}$ , so the mathematical formula of it in the mixed RF-FSO system is defined as  $P_{out}(\gamma_{th}) = \Pr(\gamma \leq \gamma_{th})$ .

Hence, the expression of outage probability can be obtained by  $P_{out}(\gamma_{th}) = F_\gamma(\gamma_{th})$ ,

$$P_{out}(\gamma_{th}) = 1 - \frac{2^{(\alpha+\beta)} A \sqrt{C}}{16\pi \sqrt{\gamma_1}} \sqrt{\gamma_{th}} \exp\left(-\frac{\gamma_{th}}{\gamma_1}\right) \times G_{6,0} \left( \frac{(\alpha\beta)^2 C \gamma_{th}}{16\gamma_1 \gamma_2} \middle| \frac{\xi^2+1}{2} \right)_{\kappa_1} \quad (5)$$

#### 3.2. Average Bit Error Rate

There are many modulations that can be used in the hybrid RF-FSO system, they have a large difference in systematic performance due to their different characteristics, such as power efficiency, bandwidth efficiency, and simplicity, the most intuitive way to evaluate the quality of a modulation method is the BER of the system.

The PPM-BPSK-SIM combines PPM and BPSK-SIM together, the symbol is modulated by a PPM encoder, then the parallel signal is transmitted to the BPSK modulator [27]. The conditional BER for various PPM is  $P_{LPPM} = \frac{1}{2} \operatorname{erfc}\left(\frac{1}{2\sqrt{2}} \sqrt{\gamma \frac{L}{2} \log_2 L}\right)$  [28–31], for L-ary pulse position modulation (LPPM), one data symbol consists of L time slots, only one time slot is valid and the rest are zero, that is, L is the average length of the symbol [28,31]. According to Equations (2) and (8) in reference [11], the definite relationship of the conditional BERs between LPPM and L-ary pulse position modulation–binary phase shift keying–subcarrier intensity modulation (LPPM-BPSK-SIM) can be derived. Utilizing  $Q(x) = \frac{1}{2} \operatorname{erfc}\left(\frac{x}{\sqrt{2}}\right)$ , the conditional BER of the LPPM-BPSK-SIM is derived as

$$P_{LPPM-BPSK-SIM} = Q\left(\frac{1}{4} \sqrt{\gamma L \log_2 L}\right). \quad (6)$$

The unconditional BER of various PPM-BPSK-SIM is obtained as

$$P_{LPPM-BPSK-SIM} = \int_0^\infty Q\left(\frac{1}{4} \sqrt{\gamma L \log_2 L}\right) f_\gamma(\gamma) d\gamma. \quad (7)$$

#### 3.3. Average Capacity

According to the definition of the average channel capacity [32,33],  $\bar{C} = E[\log_2(1 + \gamma)]$ ,  $E[\bullet]$  denotes the expectation operator, the expression for the average channel capacity of the hybrid system is given by:

$$\begin{aligned}
 C_{ave} &= \int_0^{\infty} \log_2(1 + \gamma) f_{\gamma}(\gamma) d\gamma \\
 &= \frac{1}{\ln 2} \int_0^{\infty} \frac{1}{1+\gamma} F_{\gamma}^c(\gamma) d\gamma,
 \end{aligned}
 \tag{8}$$

where  $F_{\gamma}^c(\gamma) = 1 - F_{\gamma}(\gamma)$ ,  $\frac{1}{1+\gamma} = G_{0,0}^{1,1} \left( x \middle| 0 \right)_0$ , substituting Equation (4) into Equation (8) and using the expression of the extended generalized bivariate Meijer’s G function (EGBMGF) in reference [34]. The average channel capacity is obtained as

$$C_{ave} = \frac{2^{(\alpha+\beta)} A \sqrt{C}}{16\pi \ln(2)} \gamma_1 G_{0,0:0,0:1,6}^{0,0:1,1:6,0} \left( - \middle| 0 \middle| \frac{\xi^2+1}{2} \middle| \frac{(\alpha\beta)^2 C}{16\gamma_2} \right).
 \tag{9}$$

#### 4. Results and Discussion

The performance of the mixed RF–FSO system with hybrid PPM–BPSK–SIM is shown in figures below, including outage probability performance, average BER, and average channel capacity. Note that, the RF link is assumed to obey Rayleigh distribution and we use Gamma–Gamma fading to describe the turbulence of the FSO link from weak to strong, the receiver employs IM/DD. The parameters for turbulence intensity are shown in Table 1 [35,36], the wavelength is 1550 nm, and the distance between the transmitter and the receiver is set to be 5 km.

**Table 1.** Parameters for different turbulence intensities.

Turbulence	$\alpha$	$\beta$
Weak	11.6	10.1
Moderate	4.0	1.9
Strong	4.2	1.4

The outage probability of the hybrid RF–FSO system against average SNR per hop is shown in Figure 2, effects of atmospheric turbulence and pointing errors are taken into account.  $\gamma_{th}$  is set to be 10 dB, the average SNRs of the two different links are equal to each other (i.e.,  $\bar{\gamma}_1 = \bar{\gamma}_2 = \bar{\gamma}$ ). As seen, the decrease of atmospheric turbulence leads to the improvement of the outage performance. Moreover, taking into consideration the pointing error, the greater the parameter,  $\xi$ , the better the outage performance. For instance, when the outage probability is  $P_{out} = 10^{-3}$ , the system has a 6 dB decrease on average SNR from strong turbulence to weak turbulence while  $\xi = 1$ , but the difference value is less than 0.5 dB while  $\xi = 5$ . Therefore, a conclusion is reached that pointing error aggravates the influence of atmospheric turbulence on outage probability.

Comparison diagram of average BER of BPSK in the FSO system and the hybrid RF–FSO system is shown in Figure 3. The simulation of BPSK refers to reference [37]. It can be observed that by adopting the RF link, the hybrid RF–FSO system has an improvement in BER performance compared to the FSO system. The BER of BPSK in the FSO system is lower than that in hybrid RF–FSO system, and higher average SNR of the RF channel leads to greater improvement. In order to study the performance of the hybrid RF–FSO system, we set  $\bar{\gamma}_1 = \bar{\gamma}_2 = \bar{\gamma}$  in the following.

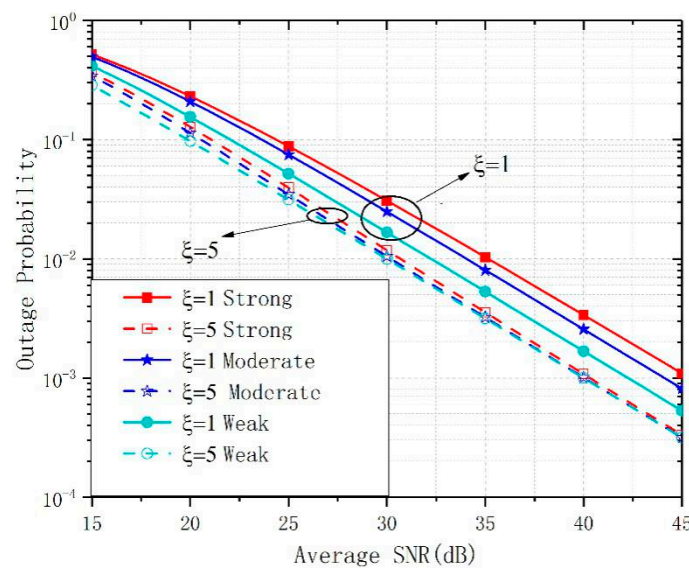


**Figure 2.** Outage probability against average signal-to-noise ratio (SNR) per hop for various turbulence intensities and different pointing error parameters. The constant is assumed to be  $C = 1$ , and the threshold of the hybrid system is  $\gamma_{th} = 10$  dB.

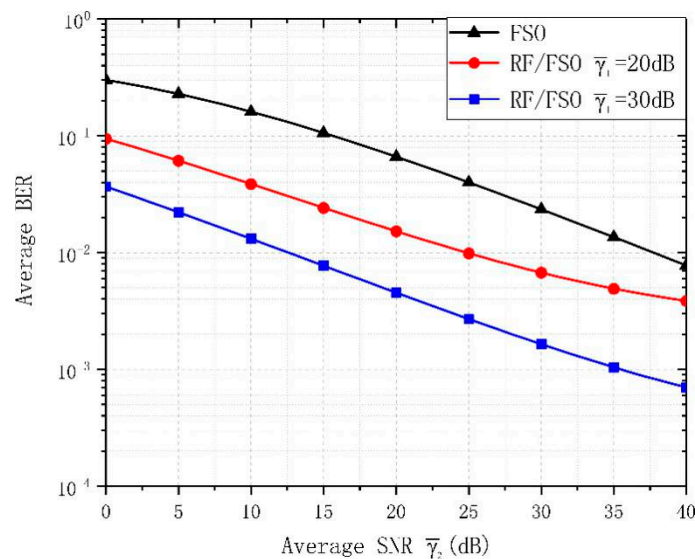


**Figure 3.** Average bit error rate (BER) of binary phase shift keying (BPSK) against average SNR under moderate turbulence and the pointing error parameter is  $\xi = 1$ . Turbulence parameters are  $\alpha = 4.0$  and  $\beta = 1.9$ , the constant is assumed to be  $C = 1$ .

Figure 4 depicts the average BER of LPPM and BPSK in the mixed RF–FSO system against the average SNR per hop, the parameter of pointing error is 1 and  $C = 1$ . It can be seen from the figure that LPPM has a better BER performance as  $L$  increases. When the value of  $L$  is greater than four, the performance of LPPM in this system is better than that of BPSK. In Figure 5, comparison between various PPM–BPSK–SIM and BPSK has been shown, the same conclusion can be drawn that the BER of the hybrid system decreases when  $L$  increases, but the marginal values are different. For instance, when the value of  $L$  is greater than eight instead of four, the hybrid system adopting various PPM–BPSK–SIM achieves better performance than the system with BPSK. Simulation results in Figure 6 show that under moderate turbulence, a decrease in the value of  $C$  causes the improvement of the average BER, but it is irrelevant to the marginal value, the PPM–BPSK–SIM outperforms BPSK when the symbol length is greater than eight, that is, this is not a special case. An increase in the symbol length will reduce



the bandwidth efficiency, which leads to an optimization of system performance for a reduction of average BER. Furthermore, the performance of the mixed modulation is affected by both modulations. Therefore, the value of  $L$  has a significant effect on the BER performance of hybrid system, the BER decreases as  $L$  increases, and the hybrid RF-FSO system achieves better BER performance by using the hybrid PPM-BPSK-SIM scheme only if the length of symbol,  $L$ , is greater than eight.

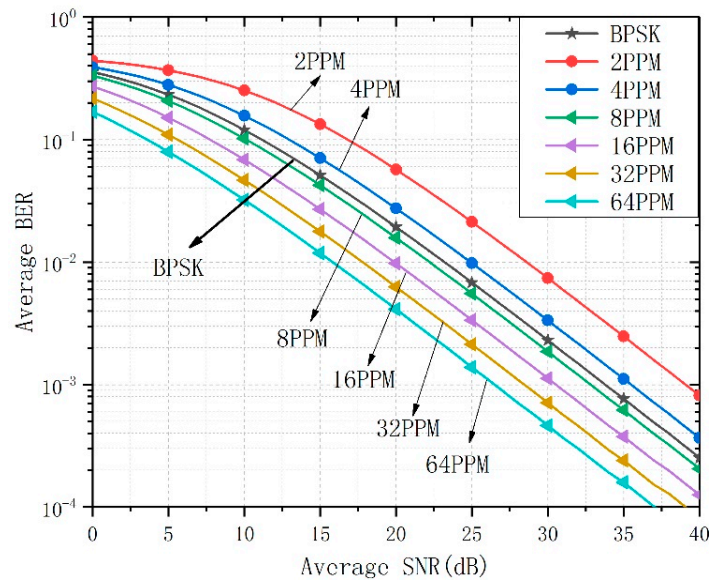


**Figure 4.** Average BER of  $L$ -ary pulse position modulation (LPPM) and BPSK against average SNR per hop under strong turbulence and the pointing error parameter is  $\xi = 1$ . Turbulence parameters are  $\alpha = 4.2$  and  $\beta = 1.4$ , the constant is assumed to be  $C = 1$ .

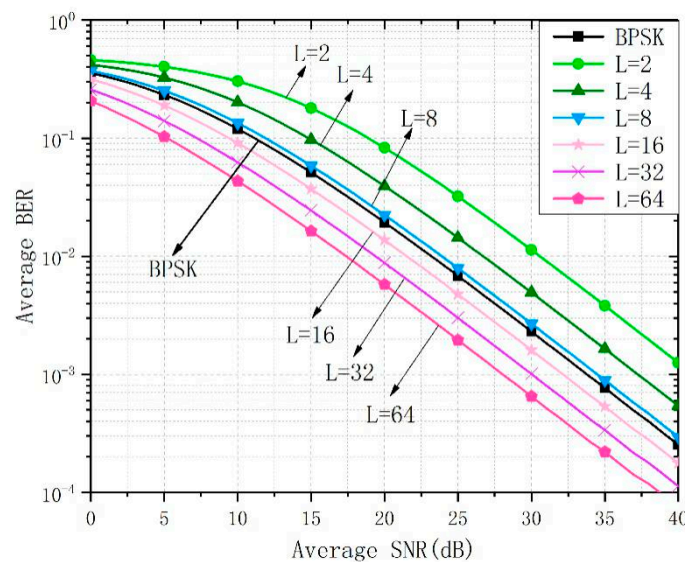


**Figure 5.** Average BER of  $L$ -ary pulse position modulation–binary phase shift keying–subcarrier intensity modulation (LPPM-BPSK-SIM) and BPSK against average SNR per hop under strong turbulence and the pointing error parameter is  $\xi = 1$ . Turbulence parameters are  $\alpha = 4.2$  and  $\beta = 1.4$ , the constant is assumed to be  $C = 1$ .

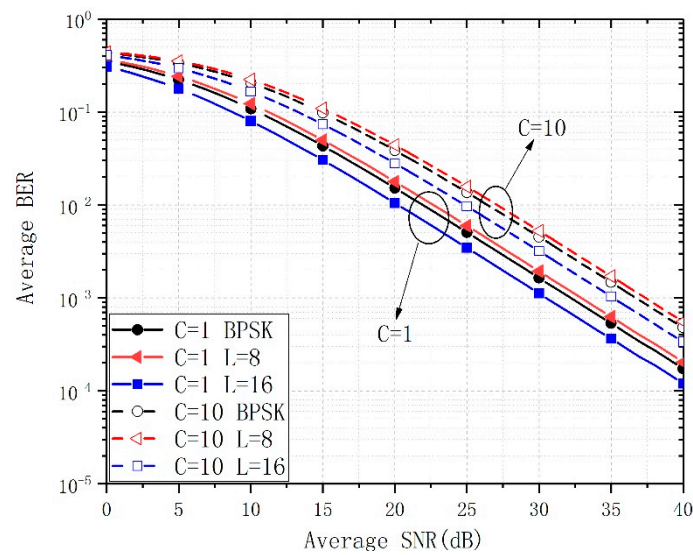


**Figure 6.** Average BER of LPPM–BPSK–SIM and BPSK against average SNR per hop under moderate turbulence and the pointing error parameter is  $\xi = 1$ . Turbulence parameters are  $\alpha = 4.0$  and  $\beta = 1.9$ .

In Figure 7, the average BERs of LPPM–BPSK–SIM, LPPM, and BPSK in the hybrid RF–FSO system are presented under the same channel condition in Figure 4, we conducted studies about  $L = 16$  and  $L = 64$ . It can be observed that when average SNR is fixed, the average BER of hybrid PPM–BPSK–SIM is higher than that of LPPM, and both of them outperform BPSK. For instance, when SNR = 25 dB, the average BER decreases in the order of BPSK, 16PPM–BPSK–SIM, 16PPM, 64PPM–BPSK–SIM, 64PPM. From another perspective, to achieve a BER of  $10^{-3}$ , 28 dB of SNR is required for 64PPM–BPSK–SIM and 32 dB is needed for 16PPM–BPSK–SIM, 33.5 dB is needed for BPSK. It can be noticed that the value of  $L$  has a great influence on the average BER of the system when using hybrid modulation, and the larger  $L$ , the lower the average BER. Considering the power efficiency and average BER of the hybrid modulation, we have conducted further research on the performance of 16PPM–BPSK–SIM.

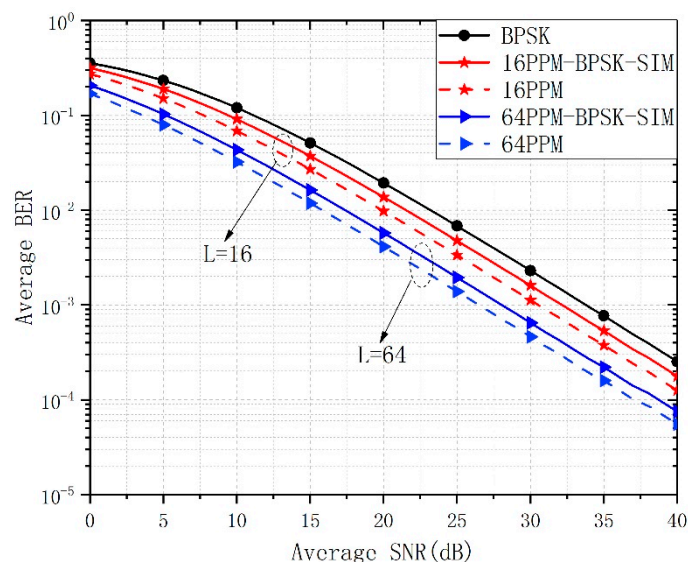


**Figure 7.** Average BER of hybrid modulation, LPPM, and BPSK against average SNR per hop under strong turbulence and the pointing error parameter is  $\xi = 1$ . Turbulence parameters are  $\alpha = 4.2$  and  $\beta = 1.4$ , the constant is assumed to be  $C = 1$ .



In Figure 8, simulations of 16PPM–BPSK–SIM under different turbulence strength and different pointing error conditions have been implemented. What can be observed easily is that pointing error has a significant influence on the average BER of the hybrid system, the average BER increases as the value of  $\xi$  decreases. For example, regardless of the intensity of turbulence, the system with  $\xi = 5$  outperforms the system with  $\xi = 1$ . On the other hand, when  $\xi$  is a fixed value, the average BER increases as the intensity of the turbulence increases, which is in line with our theoretical analysis. However, under moderate and weak turbulence with  $\xi = 5$ , the average BER of the system suddenly drops and appears to be undulating. After that, we changed the value of  $L$  and found that this condition still existed, this phenomenon indicates that the RF–FSO systematic performance is unstable. The adoption of hybrid PPM–BPSK–SIM has a stable improvement on average BER performance, especially under conditions with strong turbulence and severe pointing error.

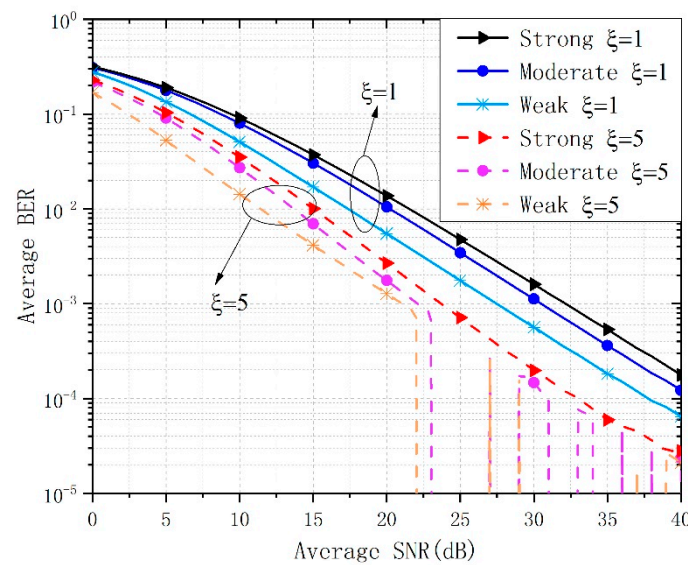


**Figure 8.** Average BER of 16PPM–BPSK–SIM against average SNR per hop for different turbulence strength and pointing error parameters. The fixed relay gain is  $C = 1$ .

In Figure 9, hybrid RF–FSO systematic average channel capacity against average SNR per hop is depicted with various turbulence intensities and different parameters of pointing error. As shown in Figure 9a, the average capacity of the system decreases with the increase of turbulence intensity regardless of the pointing error. When atmospheric turbulence strength is fixed, the larger the pointing error parameter is, the larger the system capacity will be. Further research is being carried out on the effect of pointing error on channel capacity. The differences of average capacity between strong and weak turbulence conditions are shown in Figure 9b. It can be seen from the graph that the smaller the pointing error parameter, the larger the maximum difference of average channel capacity. For instance, when  $\xi = 10$ , the maximum difference is 0.39 when SNR = 11 dB, but the maximum difference is 0.49 at SNR = 18 dB when  $\xi = 1$ . When the average SNR is greater than 11 dB, the channel capacity difference of  $\xi = 1$  is larger than that at  $\xi = 10$ , though the gap between them will gradually shrink as the SNR value increases. We can conclude that a larger pointing error parameter results in a higher channel capacity, and it can aggravate the effect on capacity caused by atmospheric turbulence.

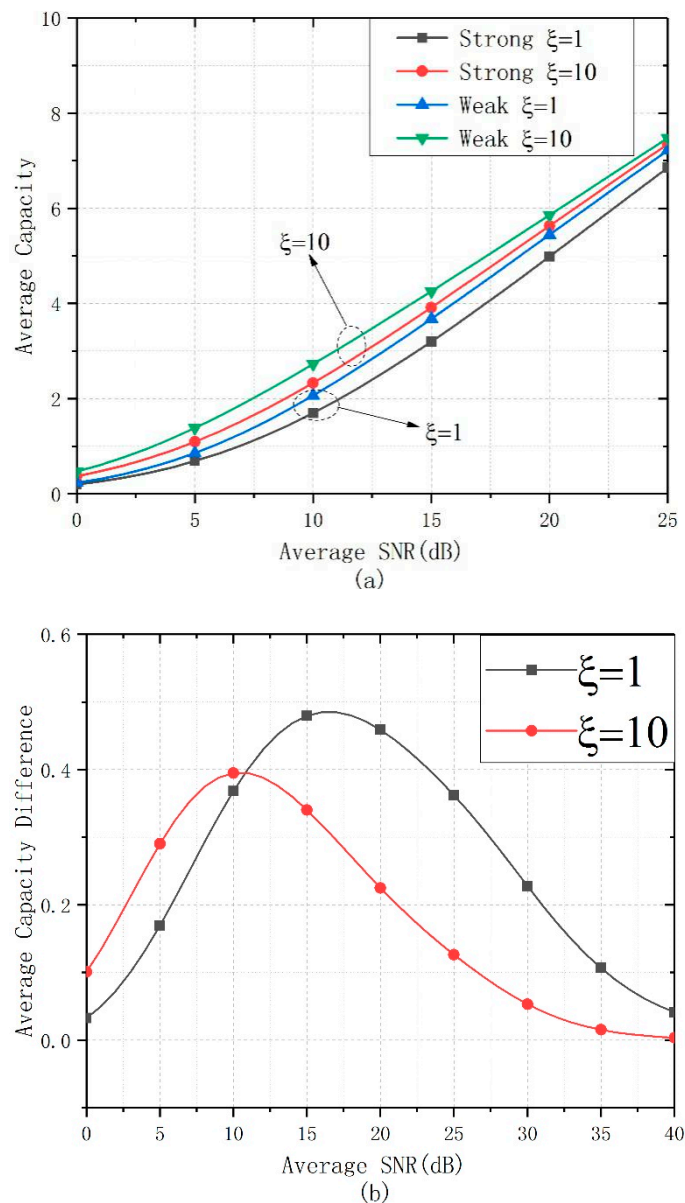


**Figure 9.** (a) Average capacity against average SNR per hop for different turbulence intensities and different pointing error parameters. (b) Average capacity difference between different pointing error parameters.

### 5. Conclusions

In summary, we studied the performance of mixed RF-FSO system with hybrid PPM-BPSK-SIM and fixed-gain relay. The RF link and the FSO link undergo Rayleigh distribution and Gamma-Gamma distribution severally. The expression of the unconditional BER of the hybrid RF-FSO system have been derived. On basis of the mathematical representation above, influences of the FSO link including atmospheric turbulence and pointing error have been investigated.

The results of our study show that the BER performance of the hybrid system could be ameliorated when it adopts hybrid PPM-BPSK-SIM, and the specific improvement effect has a lot to do with the length of symbol,  $L$ . The BER of the hybrid system degrades as the value of  $L$  increases, and when  $L$  is greater than eight, the hybrid system has a better BER performance than BPSK. The hybrid PPM-BPSK-SIM can improve the performance of the mixed RF-FSO system stably and obviously with strong turbulence and severe pointing error conditions. The outage probability and the average

channel capacity are sensitive to turbulence effect and pointing error of the FSO channel. Simulation results also indicate that the pointing error can aggravate the effect of atmospheric turbulence on channel capacity and outage probability. Thus, the performance of mixed RF-FSO system could be improved by adopting hybrid PPM-BPSK-SIM, especially under conditions with strong turbulence influence and severe pointing error effect.

**Author Contributions:** Conceptualization: H.L.; formal analysis and writing: T.J.; investigation: L.Z.; methodology: X.Y.; validation: D.D. and A.L.; software: Z.W.

**Funding:** This study was funded by the National Natural Science Foundation of China; grant numbers are 61875057 and 61475049.

**Conflicts of Interest:** The authors declare no conflict of interest.

## References

1. Lorences-Riesgo, A.; Guiomar, F.P.; Sousa, A.N.; Teixeira, A.L.; Muga, N.J.; Monteiro, P.P. 200 Gbit/s Free-Space Optics Transmission Using a Kramers-Kronig Receiver. In Proceedings of the Optical Fiber Communication Conference (OFC) 2019, San Diego, CA, USA, 3 March 2019.
2. Song, H.; Song, H.; Zhang, R.; Manukyan, K.; Li, L.; Zhao, Z.; Pang, K.; Liu, C.; Almainan, A.; Bock, R.; et al. Experimental Mitigation of Atmospheric Turbulence Effect using Pre-Channel Combining Phase Patterns for Uni- and Bidirectional Free-Space Optical Links with Two 100-Gbit/s OAM-Multiplexed Channels. In Proceedings of the Optical Fiber Communication Conference Postdeadline Papers 2019, San Diego, CA, USA, 3 March 2019.
3. Gupta, J.; Dwivedi, V.K.; Karwal, V. On the Performance of RF-FSO System Over Rayleigh and Kappa-Mu/Inverse Gaussian Fading Environment. *IEEE Access* **2018**, *6*, 4186–4198. [[CrossRef](#)]
4. Anees, S.; Bhatnagar, M.R. Performance of an amplify-and-forward dual-hop asymmetric RF-FSO communication system. *J. Opt. Commun. Netw.* **2015**, *7*, 124–135. [[CrossRef](#)]
5. Samimi, H.; Uysal, M. End-to-end performance of mixed RF/FSO transmission systems. *IEEE/OSA J. Opt. Commun. Netw.* **2013**, *5*, 1139–1144. [[CrossRef](#)]
6. Zhang, J.; Dai, L.; Zhang, Y.; Wang, Z. Unified performance analysis of mixed radio frequency/free-space optical dual-hop transmission systems. *J. Lightwave Technol.* **2015**, *33*, 2286–2293. [[CrossRef](#)]
7. Zhang, Y.; Wang, X.; Zhao, S.-H.; Zhao, J.; Deng, B.-Y. On the performance of  $2 \times 2$  DF relay mixed RF/FSO airborne system over Exponentiated Weibull fading channel. *Opt. Commun.* **2018**, *425*, 190–195. [[CrossRef](#)]
8. Petkovic, M.I.; Ansari, I.S.; Djordjevic, G.T.; Qaraqe, K.A. Error rate and ergodic capacity of RF-FSO system with partial relay selection in the presence of pointing errors. *Opt. Commun.* **2019**, *438*, 118–125. [[CrossRef](#)]
9. Zhao, J.; Zhao, S.-H.; Zhao, W.-H.; Liu, Y.; Li, X. Performance of mixed RF/FSO systems in exponentiated Weibull distributed channels. *Opt. Commun.* **2017**, *405*, 244–252. [[CrossRef](#)]
10. Torabi, M.; Effatpanahi, R. Performance analysis of hybrid RF-FSO systems with amplify-and-forward selection relaying. *Opt. Commun.* **2019**, *434*, 80–90. [[CrossRef](#)]
11. Faridzadeh, M.; Gholami, A.; Ghassemlooy, Z.; Rajbhandari, S. Hybrid PPM-BPSK subcarrier intensity modulation for free space optical communications. In Proceedings of the 2011 16th European Conference on Networks and Optical Communications (NOC), Newcastle, UK, 20–22 July 2011; pp. 36–39.
12. Giri, R.K.; Patnaik, B. BER analysis and capacity evaluation of FSO system using hybrid subcarrier intensity modulation with receiver spatial diversity over log-normal and gamma-gamma channel model. *Opt. Quantum Electron.* **2018**, *50*, 231. [[CrossRef](#)]
13. Ansari, I.S.; Yilmaz, F.; Alouini, M.-S. Impact of pointing errors on the performance of mixed RF/FSO dual-hop transmission systems. *IEEE Wirel. Commun. Lett.* **2013**, *2*, 351–354. [[CrossRef](#)]
14. Zedini, E.; Ansari, I.S.; Alouini, M.-S. Performance analysis of mixed Nakagami- $m$  and Gamma-Gamma dual-hop FSO transmission systems. *IEEE Photonics J.* **2014**, *7*, 1–20. [[CrossRef](#)]
15. Prabu, K.; Kumar, D.S.; Srinivas, T. Performance analysis of FSO links under strong atmospheric turbulence conditions using various modulation schemes. *Opt. Int. J. Light Electron Opt.* **2014**, *125*, 5573–5581. [[CrossRef](#)]

16. Xu, F.; Lau, F.C.; Yue, D.-W. Diversity order for amplify-and-forward dual-hop systems with fixed-gain relay under Nakagami fading channels. *IEEE Trans. Wirel. Commun.* **2010**, *9*, 92–98. [[CrossRef](#)]
17. Aggarwal, M.; Garg, P.; Puri, P. Dual-hop optical wireless relaying over turbulence channels with pointing error impairments. *J. Lightwave Technol.* **2014**, *32*, 1821–1828. [[CrossRef](#)]
18. Ansari, I.S.; Yilmaz, F.; Alouini, M.-S. Performance analysis of FSO links over unified Gamma-Gamma turbulence channels. In Proceedings of the 2015 IEEE 81st Vehicular Technology Conference (VTC Spring), Glasgow, Scotland, 11–14 May 2015; pp. 1–5.
19. Bhatnagar, M.R.; Ghassemlooy, Z. Performance evaluation of FSO MIMO links in Gamma-Gamma fading with pointing errors. In Proceedings of the 2015 IEEE International Conference on Communications (ICC), London, UK, 8–12 June 2015; pp. 5084–5090.
20. Liu, C.; Yao, Y.; Sun, Y.; Zhao, X. Analysis of average capacity for free-space optical links with pointing errors over gamma-gamma turbulence channels. *Chin. Opt. Lett.* **2010**, *8*, 537–540.
21. Trung, H.D.; Pham, A.T. Pointing error effects on performance of free-space optical communication systems using SC-QAM signals over atmospheric turbulence channels. *AEU-Int. J. Electron. Commun.* **2014**, *68*, 869–876. [[CrossRef](#)]
22. Yang, L.; Gao, X.; Alouini, M.-S. Performance analysis of relay-assisted all-optical FSO networks over strong atmospheric turbulence channels with pointing errors. *J. Lightwave Technol.* **2014**, *32*, 4613–4620. [[CrossRef](#)]
23. Gradshteyn, I.S.; Ryzhik, I.M. *Table of Integrals, Series, and Products*; Academic Press: Cambridge, MA, USA, 2014.
24. Al-Eryani, Y.F.; Salhab, A.M.; Zummo, S.A.; Alouini, M.-S. Two-way multiuser mixed RF/FSO relaying: Performance analysis and power allocation. *IEEE/OSA J. Opt. Commun. Netw.* **2018**, *10*, 396–408. [[CrossRef](#)]
25. Adamchik, V.; Marichev, O. The algorithm for calculating integrals of hypergeometric type functions and its realization in REDUCE system. In Proceedings of the International Symposium on Symbolic and Algebraic Computation, Tokyo, Japan, 20–24 August 1990; pp. 212–224.
26. Hasna, M.O.; Alouini, M.-S. A performance study of dual-hop transmissions with fixed gain relays. *IEEE Trans. Wirel. Commun.* **2004**, *3*, 1963–1968. [[CrossRef](#)]
27. Faridzadeh, M.; Gholami, A.; Ghassemlooy, Z.; Rajbhandari, S. Hybrid pulse position modulation and binary phase shift keying subcarrier intensity modulation for free space optics in a weak and saturated turbulence channel. *JOSA A* **2012**, *29*, 1680–1685. [[CrossRef](#)]
28. Elganimi, T.Y. Performance comparison between OOK, PPM and pam modulation schemes for free space optical (FSO) communication systems: Analytical study. *Int. J. Comput. Appl.* **2013**, *79*. [[CrossRef](#)]
29. Faridzadeh, M.; Gholami, A.; Ghassemlooy, Z.; Rajbhandari, S. Hybrid 2-PPM-BPSK-SIM with the spatial diversity for free space optical communications. In Proceedings of the 2012 8th International Symposium on Communication Systems, Networks & Digital Signal Processing (CSNDSP), Poznan, Poland, 18–20 July 2012; pp. 1–5.
30. Trisno, S. Design and Analysis of Advanced Free Space Optical Communication Systems. Ph.D. Thesis, University of Maryland, College Park, MD, USA, 2006.
31. Yi, X.; Liu, Z.; Yue, P.; Shang, T. BER performance analysis for M-ary PPM over gamma-gamma atmospheric turbulence channels. In Proceedings of the 2010 6th International Conference on Wireless Communications Networking and Mobile Computing (WiCOM), Chengdu, China, 23–25 September 2010; pp. 1–4.
32. Si, C.; Zhang, Y.; Wang, Y.; Wang, J.; Jia, J. Average capacity for non-Kolmogorov turbulent slant optical links with beam wander corrected and pointing errors. *Opt. Int. J. Light Electron Opt.* **2012**, *123*, 1–5. [[CrossRef](#)]
33. Annamalai, A.; Palat, R.; Matyjas, J. Estimating ergodic capacity of cooperative analog relaying under different adaptive source transmission techniques. In Proceedings of the 2010 IEEE Sarnoff Symposium, Princeton, NJ, USA, 12–14 April 2010; pp. 1–5.
34. Ansari, I.S.; Al-Ahmadi, S.; Yilmaz, F.; Alouini, M.-S.; Yanikomeroglu, H. A new formula for the BER of binary modulations with dual-branch selection over generalized-K composite fading channels. *IEEE Trans. Commun.* **2011**, *59*, 2654–2658. [[CrossRef](#)]
35. Popoola, W.O.; Ghassemlooy, Z. BPSK subcarrier intensity modulated free-space optical communications in atmospheric turbulence. *J. Lightwave Technol.* **2009**, *27*, 967–973. [[CrossRef](#)]

36. Ghassemlooy, Z.; Popoola, W.; Rajbhandari, S. *Optical Wireless Communications: System and Channel Modelling with Matlab®*; CRC Press: Boca Raton, FL, USA, 2019.
37. Chatzidiamantis, N.D.; Karagiannidis, G.K.; Kriezis, E.E.; Matthaiou, M. Diversity combining in hybrid RF/FSO systems with PSK modulation. In Proceedings of the 2011 IEEE International Conference on Communications (ICC), Kyoto, Japan, 5–9 June 2011; pp. 1–6.



© 2019 by the authors. Licensee MDPI, Basel, Switzerland. This article is an open access article distributed under the terms and conditions of the Creative Commons Attribution (CC BY) license (<http://creativecommons.org/licenses/by/4.0/>).